Dynamics of spiral waves in excitable media subjected to external periodic forcing

A. Schrader, M. Braune, and H. Engel
Institut für Theoretische Physik, Technische Universität Berlin, Rudower Chaussee 5, Haus 2.14, D-12489 Berlin, Germany
(Received 16 August 1994)

We provide a survey of the behavior of meandering spiral waves in excitable media under periodic modulation of excitability. Model calculations were performed in a modified Oregonator model for the photosensitive Belousov-Zhabotinsky reaction. The spiral's dynamic is followed by its tip motion. We find mode locking if the path curvature period is a rational multiple of the modulation period and resonance response of the spiral's rotation period. A general ordering structure in terms of the Farey tree is observed. The complex motion of the spiral's tip is found to be composed of harmonics of the modulation period. For large forcing amplitudes we observe an overlap of entrainment bands resulting in bistable behavior and in the breakup of the spiral at the end of the major entrainment band.

PACS number(s): 82.40.Ck, 82.20.Wt, 87.90.+y

I. INTRODUCTION

Traveling waves of excitation are well-known examples of the spontaneous formation of spatiotemporal structures in distributed active media. Spiral waves in two spatial dimensions have attracted much attention. They have been observed in active media of quite different natures: circulating waves of neuromuscular activity in the heart muscle, where they were associated with cardiac arhythmia [1]; cAMP (cyclic adenosine-monophosphate) waves in social amoeba colonies, where they control the chemotactic cell motion [2]; spiral waves of intracellular calcium release, where signals are mediated through Ca^{2+} by a multitude of hormone receptors [3]; chemical waves, as in coverage patterns during the catalytic oxidation of carbon monoxide on platinum single crystal surfaces under ultrahigh vacuum conditions [4] or spiral waves of chemical activity in the Belousov-Zhabotinskii (BZ) reaction [5,6].

The BZ reaction is certainly the most extensively studied system that supports spiral waves. A photosensitive modification of this reaction that uses the catalytic complex rutheniumbipyridyl [Ru(bpy)] provides a suitable tool to examine the response of spiral waves to external forcing experimentally [7]. Since rutheniumbipyridyl is light sensitive, the excitability of the medium may be controlled by the intensity of the applied illumination. Periodic modulation of the light intensity gives way to a large variety of complex dynamical behavior [8–10]. The detailed chemical changes in the active medium during illumination are still unknown. In 1990 Krug, Pohlmann, and Kuhnert proposed a simple modification of the well-known Oregonator model of the BZ reaction, which accounts for an additional inhibitor flow produced photochemically [11]. These modified Oregonator equations are the basis of our numerical calculations.

In the simplest case, spiral waves rotate rigidly around a fixed circular center, the spiral's core, with constant rotation frequency ω_0. Outside this core the medium is periodically excited with $T_0=2\pi/\omega_0$. The path of the spiral's tip describes a perfect circle. However, rigidly rotating spirals are rather an exception. More generally, the dynamic of spiral waves is described by a noncircular, two-frequency compound motion called meandering [6]. Meandering motion is a generic feature of excitable media. It occurs as a Hopf bifurcation from rigid rotation as a control parameter is varied [12,13]. Meandering means that the spiral's tip is looping around a temporally changing center. The path of the spiral tip describes a flowerlike pattern. Therefore, we refer to meander patterns as flowers composed of loops or petals. The variation of excitability parameters leads through a flower garden of tip path patterns [14,15]. The stationary meander regime has already been intensively studied both experimentally [12,16–20] and theoretically [13–15,21–24].

Recently, special interest has been focused on the dynamics under nonstationary conditions in order to gain new insights of wave propagation in active media in general and possibly to control the spiral's behavior. The medium's properties can be varied by periodic perturbation of the excitability. In the photosensitive BZ reaction, periodic modulation of the applied light intensity gives way to a larger variety of complex meander patterns. Moving flowers, patterns with different petal sizes, and quite irregular patterns were found experimentally in good qualitative agreement with numerical results. The fundamental characteristics of the system under periodic modulation, i.e., entrainment bands and resonances, have already been reported in a previous paper [9]. Here we present additional numerical results. More complex structures have been investigated and mode-locked states were found to obey the hierarchical ordering of the Farey tree. We then discuss the behavior on the main entrainment bands with emphasis on the beginning and termination of the bands. Furthermore, we draw attention to resonance response accompanied by synchronization due to large forcing amplitudes. We also observe interesting phenomena, such as bistability due to overlapping entrainment bands and an instability leading to the breakup of the spiral.

II. THE OREGONATOR MODEL AND COMPUTATIONAL PROCEDURE

For spatially extended BZ media the two-variable version of the Oregonator reads [25]

 ©1995 The American Physical Society

$$\frac{\partial u}{\partial t}=\frac{1}{\epsilon}\left[u(1-u)-fv\left[\frac{u-q}{u+q}\right]\right]+D_u\Delta u\ ,$$
$$\frac{\partial v}{\partial t}=u-v+D_v\Delta v\ . \tag{1}$$

$u(\vec{x},t)$ presents the reaction variable, while $v(\vec{x},t)$ is a control variable. The variables u and v are related to the local concentrations by the following scaling relations:

$$u=\left[\frac{2k_4}{k_3A}\right]U,\quad v=\left[\frac{k_4k_5B}{(k_3A)^2}\right]V\ .$$

Here U and V are the concentrations in moles per liter of bromous acid and the oxidized form of the metal ion catalyst, respectively. Rate constants are given by k_1 through k_5. $A=[BrO_3^-]$ and $B=[MA+BrMA]$ (MA denotes malonic acid) are assumed to be constant concentrations. Time is scaled as $t=k_5BT$, with T the time in seconds. The small parameter $q=2(k_1k_4/k_2k_3)$ depends only on rate constants and has been estimated to be between 0.0002 and 0.002 [14]. The parameter f defined as $2h$ presents the excitation threshold, where h is a stoichiometric coefficient; it measures the amount of Br^- produced per unit of the reduced form of the metal ion catalyst Me(ox):

$$MA+BrMA+Me(ox)\rightarrow hBr^-\ . \tag{2}$$

The time-scale factor $\epsilon=k_5B/k_3A$ is estimated to be $\epsilon\approx10^{-2}$ and presents the ratio of the rate of recovery to the rate of excitation [25]. With the choice of $D_u=1$, space units are scaled to $\sqrt{D/k_5B}$, where D is the physical diffusion coefficient of $HBrO_2$. The ratio D_v/D_u can be estimated from the molecular weights of $HBrO_2$ and the catalyst.

The two-variable Oregonator has solutions that represent propagation of wave fronts by the interplay of $HBrO_2$ diffusion with an autocatalytic reaction, which quickly generates $HBrO_2$, while Br^- is assumed to always remain in equilibrium with the local instantaneous $HBrO_2$. The recovery process is mediated by the metal ion catalyst, which has been a cerium complex in the original Oregonator scheme.

If the catalyst is changed to the light-sensitive ruthenium complex $Ru(bpy)_3$, where bpy $=2,2'$-bipyridyl, an additional constant bromide flow Φ is observed under constant illumination. Without illumination the reduced Ru complex promotes the autocatalytic production of the bromic acid:

$$2Ru^{2+}+HBrO_3+HBrO_2+2H^+\rightarrow2Ru^{3+}+2HBrO_2+H_2O\ . \tag{3}$$

According to Kuhnert [26] illumination creates an excited state of the ruthenium complex $Ru^{2+}\rightarrow Ru^{2+*}$. This excited complex rapidly reduces BrO_3^- to Br^-:

$$6Ru^{2+*}+BrO_3^-+6H^+\rightarrow6Ru^{3+}+3H_2O+Br^-\ . \tag{4}$$

From this simplified view of the chemical mechanism, visible light influences the ruthenium catalyzed BZ reaction Krug, Pohlmann, and Kuhnert proposed to include an additional flow term into the equation of the bromide balance [11]. It is assumed that the velocity of the additional bromide release is proportional to the light intensity. In consequence, the two-variable Oregonator model is modified to

$$\frac{\partial u}{\partial t}=\frac{1}{\epsilon}\left[u(1-u)-(fv+\phi)\left[\frac{u-q}{u+q}\right]\right]+D_u\Delta u\ ,$$
$$\frac{\partial v}{\partial t}=u-v+D_v\Delta v\ , \tag{5}$$

where the photochemically produced bromide flow Φ is scaled as $\phi=[2k_4/(k_3A)^2]\Phi$. Periodic forcing of excitability is introduced into the Oregonator model by the modulation of the additional ϕ term, which corresponds to the light intensity in the BZ reaction

$$\phi(t)=\phi_0+a\cos(2\pi t/T_{\text{mod}})\ , \tag{6}$$

where T_{mod} is the modulation period and a the forcing amplitude. We choose ϕ_0 to be 0.01 and fix $q=0.002$ and the ratio of diffusion coefficients $D_v/D_u=0.6$.

Our computations are carried out for $\epsilon=0.01$ and three values of the parameter f. $\epsilon=0.01$ comes closest to Tyson's estimate for the Oregonator model [25]. Values of f were chosen such that the patterns compare qualitatively to those obtained in experiments [8]. Because of the uncertainty of the chemical meaning of f, quantitative comparisons are very difficult. An additional criterion has been to be far away from any boundary where meandering spiral waves become unstable. We choose $f=2.5$, 2.7, and 3.0 in combination with three different forcing amplitudes $a=0.004$, 0.006, and 0.008. These choices assure that the local kinetics always remain in the excitable regime. Different values of f are used in order to distinguish between "general" behavior and behavior dependent on the system parameters. The modulation period T_{mod} is increased in steps in the range 0.4 and 3.1, or 4.7 (in the case $f=2.7$ and $a=0.008$) in dimensionless Oregonator time units. We choose step sizes of ΔT_{mod} between 0.1 and 0.05 to obtain an overall picture. However, it is chosen to be much smaller in some particularly interesting regions.

System (5) is integrated in two spatial dimensions programmed in FORTRAN. The time derivatives are substituted by differences using an explicit Euler method. The Laplacian in (5) is calculated by a five-point discretization, that is, considering only the four nearest neighbors of each grid point. In order to avoid a numerical instability, the following condition has to be fulfilled when using the five-point Laplacian: $\Delta t\leq(\Delta h)^2/4D_u$. Appropriate time steps Δt and grid spacings Δh fulfilling these conditions have been chosen to be $\Delta t=0.001$ and $\Delta h=0.125$ in most cases. However, in some "critical" cases, $\Delta h=0.075$ has been used. In none of these cases did a finer time step affect the solutions. A box size of 280×280 grid points corresponding to a length L of 35 spatial units was usually sufficient; only for strongly drifting spirals or at the spiral breakup has it been increased to 340×340 or even 560×560 meshes. At the walls of the box zero-flux (Neumann) boundary conditions have been applied.

Rotating spirals were initially created as suggested in [16]. In most cases under periodic modulation, spirals created without forcing served as initial conditions. However, to detect an overlap of entrainment bands it has been necessary to use previously modulated spirals with slightly increased or decreased modulation period as initial conditions.

Following Jahnke and Winfree [14] we define the spiral's tip to be the geometrical center of grid points occupied by intermediate u and v values. An alternative definition (i.e., the intersection of constant concentration lines) has been tested and did not alter the results. The essential characteristics of the tip path patterns are curvature changes in time. The curvature is calculated according to its definition in Cartesian coordinates,

$$K(t)=\frac{\dot{x}\ddot{y}-\dot{y}\ddot{x}}{(\dot{x}^2+\dot{y}^2)^{3/2}} . \tag{7}$$

For numerical differentiation a simple centered differences algorithm is applied. However, the calculated tip data were not smooth enough to proceed directly. They were first interpolated by a cubic spline polynomial. Then a discrete Fourier transform (DFT) was applied to the so-calculated curvature time series to obtain the period of curvature changes.

III. MEANDERING MOTION OF SPIRAL WAVES—BASIC FREQUENCIES AND CURVATURE CHANGES

The spiral's rotation period T_0 is unambiguously defined only in the case of rigidly rotating spirals. In the case of compound rotation of meandering spiral waves the period of excitation depends strongly on the location where it is measured. Using spatially fixed detectors to measure the activator concentration above a certain level mainly gives three answers at three different locations. A detector placed far outside the center measures the rotation period of the spiral arm which is no longer sensitive to the meandering of the spiral tip. We call this period T_1. Directly inside the center the period of the spiral's tip curvature modulation is detected, which corresponds to the average time the tip needs to perform a single petal of the meander flower. Therefore, we choose the name T_{loop} for this period. Close to the spiral's center but still outside, concentration time series are strongly modulated, absolute concentration maxima or minima are detected at intervals of some T_2, while the average interval of all peaks still corresponds to T_1.

Consider an n-petaled flower that is completed once during the secondary rotation period T_2. The medium is excited $(n-1)$ times outside the pattern during the period T_2. Therefore we have $f_1=1/T_1=n-1$ and $f_2=1/T_2=1$. On the other hand, the spiral's tip crosses the center n times, tracing out n petals. Thus the path curvature frequency $f_{\text{loop}}=1/T_{\text{loop}}=n$ is the sum of f_1 and f_2. In general, a closed pattern is obtained if the frequency ratio is some rational number $f_1/f_2=p/q$, in which case the $(p+q)/q$ is equal to the number of loops $n=T_2/T_{\text{loop}}$ or regions of maximum curvature per rotation of the secondary period. That $T_{\text{loop}}=1/(f_1+f_2)$ holds more generally is shown below by comparing the tip trajectory to an epicycle.

For some "regular" meander pattern the tip trajectory may be approximated by an epicycle, which describes the path of the radius vector of one circle rotating with $2\pi f_1$ centered on another circle rotating with $2\pi f_2$ [9,12,20,27,28]. If the senses of rotation are oppositely directed the typical outward meander patterns are obtained, i.e., the points of maximum curvature lie outside the flower. In Cartesian coordinates the epicycle trajectory is given by

$$\begin{aligned} x(t)&=a\cos(2\pi f_1 t)+b\cos(2\pi f_2 t) , \\ y(t)&=a\sin(2\pi f_1 t)-b\sin(2\pi f_2 t) , \end{aligned} \tag{8}$$

where a and b denote the radii of the circles. The ratio of the radii determines the petal size and the size of the core region; that is, the center of the pattern. In order to prove that $T_{\text{loop}}=1/(f_1+f_2)$ corresponds to the curvature variation, we calculate the epicycle curvature by simply plugging in the epicycle equations (8) into Eq. (7) and differentiate with respect to time. The result is that the curvature of the epicycle trajectory changes with the sum of the frequencies and is maximal for $t=T_{\text{loop}}=1/(f_1+f_2)$, not only in the cases of a rational frequency ratio.

In general, there are two different ways to determine the characteristic frequencies of the compound rotation. First, the epicycle frequencies f_1 and f_2 are observed in the Fourier spectra of the tip trajectory and detectable in modulated time series close to the center [12]. Second, T_1 is detected as the spiral arm's rotation period and T_{loop} as the averaged curvature variation of the tip trajectory. Both modes of description are absolutely equivalent, at least as long as the epicycle picture holds. However, we found that $T_{\text{loop}}=1/(f_1+f_2)$, the average time the spiral tip needs to perform a single loop or petal, corresponds to the average time of successive curvature maxima of the tip path, even for patterns where the comparison to epicycles breaks down.

We determine T_{loop} from the Fourier spectra of the curvature time series. The result is compared to the sum of the major frequencies in the Fourier spectra of the tip trajectory. An alternative method, as used in the experiments, is simply to observe the tip path, try to find a reoccurring pattern, measure the time difference, and divide it by the number of loops. Results obtained in this way can be checked by stroboscopic plots of the tip path with the period of the estimated T_{loop}. The resulting points should be found on parts of the pattern with comparable curvature.

In order to determine T_1, the simple detector method is used. For better accuracy, we placed four detectors far outside the spiral center that detect the activator concentration above a certain level. Since the resulting time series are dependent on the position of the detectors relative to the spiral center, which is not always predictable in advance, long time averages are needed in order to calculate an averaged T_1. These results are compared with

the Fourier spectra from the tip path and in most cases are found to be in good agreement.

IV. NUMERICAL RESULTS

In general, periodic forcing introduces a third frequency into the system, which results in additional curvature variations at the spiral's tip, in variations of the width of the spiral arm and of the maximum activator concentration. Variations of the spiral's width are more pronounced for slow forcing, i.e., large T_{mod}. The basic frequencies observed in the Fourier spectra of the tip path f_1, f_2, and f_3 are $f_1=1/T_1$, $f_2=f_{\mathrm{loop}}-f_1=1/T_2$, and $f_3=f_{\mathrm{mod}}-f_1=1/T_3$. Their ratios and their amplitude ratios determine the structure of the meander patterns.

The finding of pronounced entrainment bands if the path curvature period T_{loop} is a rational multiple of the modulation period T_{mod} has already been reported in [9]. On the $T_{\mathrm{mod}}/T_{\mathrm{loop}}=1/n$ entrainment bands (with $n=1,2,3$) the system is reduced to an effective two-frequency system and we obtain simple meander flowers, which compare to epicycles that are similar to those found in unperturbed systems. Our observations are in accordance with those in [10,28].

Here, we additionally investigate the structure of more complex tip path patterns obtained under periodic modulation of excitability and discuss the spiral's tip dynamic leading to mode-locked states in $T_{\mathrm{mod}}/T_{\mathrm{loop}}$ in terms of curvature variations. Two characteristic examples for small ($a=0.004$) and large ($a=0.008$) forcing amplitudes are shown in Figs. 1(a) and 1(b), which present the main numerical results in terms of the response of the internal periods to the periodic external forcing. The corresponding unforced patterns contain between three and four petals per secondary rotation T_2.

The 1/1 entrainment bands are the most pronounced in all cases. Additional entrainment bands are obtained preferably in the superharmonic region ($T_{\mathrm{mod}}/T_{\mathrm{loop}}<1$); in particular, a pronounced 1/2 band is found. There are also indications for 3/2 and 2/1 bands, which have, however, a comparably smaller width. For large forcing amplitude [Fig. 1(b)] a 5/2 band was still resolvable. However, many states, which appear only as single points on these curves, could be identified as entrained by periodic forcing and serve as an indicator for the structure of the meander patterns. This will be shown in comparing the curvature time series to the periodic modulation in the following section.

In the case of large forcing amplitudes, Fig. 1(b) reveals two additional characteristic features of the system. First, it is shown that an overlap between the 1/2 and 1/1 entrainment bands appears, which results in bistable behavior. Furthermore, a different kind of spiral wave instability in this system, which results in the breakup of the spiral, occurs at the end of the 1/1 entrainment. The bands terminate with a resonance between T_{mod} and T_1 for $a=0.008$; compare below with Sec. IV A. This also explains the absence of the 3/2 band on this curve. Here the value of T_{loop} comes very close to that of T_1. Note that the values of T_1 at the end of the 1/1 entrainment band are only rough estimates, since in this region the instability leading to the spiral breakup occurs.

The beginning of the entrainment bands can be identified by an additional decrease of the periods T_1 and

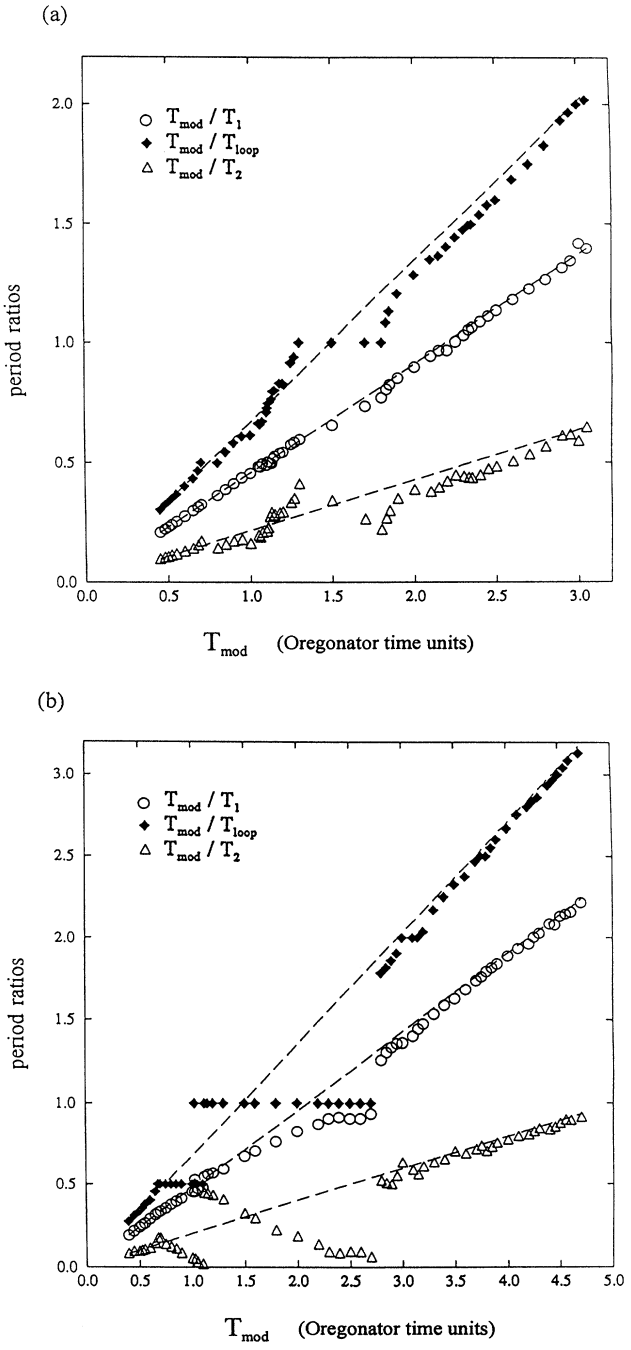

FIG. 1. Response of the internal periods to periodic modulation. Period ratios $T_{\mathrm{mod}}/T_{\mathrm{loop}}$ (diamonds), T_{mod}/T_1 (circles), and T_{mod}/T_2 (triangles) versus T_{mod}. Numerical results are shown for two different values of the f parameter and different forcing amplitudes a. (a) $f=3.0$, $a=0.004$. (b) $f=2.7$, $a=0.008$, all other parameters are fixed, i.e., $\epsilon=0.01$, $D_v/D_u=0.6$, $\phi=0.01$. The dashed lines indicate the period ratios of the corresponding unperturbed patterns.

T_{loop} below the value of the corresponding unperturbed patterns. On the band the periods increase significantly with increasing T_{mod} and drop sharply when the bands terminate. However, the values of the unperturbed patterns are not quite reached again beyond the 1/1 band for larger T_{mod}; see also Fig. 3(b) in [9]. The width of the major bands is increasing with the forcing amplitude, as expected from the theory of forced oscillators [29].

A. Mode-locked states and Farey tree structure

In the following we try to classify the observed meander patterns by their locking ratios T_{mod}/T_{loop}. The locking ratio is determined from the curvature time series in comparison to the modulation period and its Fourier spectrum (DFT). The value of T_{loop} is compared in all cases to the sum of the dominant frequencies in the Fourier spectrum [fast Fourier transform (FFT)] of the tip path itself [meaning $x(t)$ or $y(t)$] and found to be in good agreement.

Flowers corresponding to p/q mode-locked states with $T_{mod}=p/qT_{loop}$, $p>1$ consist of petals with different sizes and shapes that reoccur following certain regular patterns. We call these flowers *composed flowers* and the parts of the composition *subflowers*.

The dominating frequencies in the FFT of the tip path are still f_1 and f_2, and the averaged T_{loop} still corresponds to the sum. However, now T_{loop} is composed of two different loop periods, which are seen to be a linear combination of T_{mod} and/or its harmonics. Both the structure of the tip path pattern and the composition of T_{loop} in terms of T_{mod} and its harmonics obey the ordering of the Farey tree, which organizes the devil's staircase [27,29,30]. In particular, we found that for all patterns corresponding to locked modes p/q in the superharmonic ($T_{mod}/T_{loop}<1$) regime between $1/k$ and $1/(k-1)$, where kT_{mod} is a harmonic of T_{mod} (for the observed values $k=2,3,4$), the following relation holds:

$$pT_{loop}=a(kT_{mod})+b[(k-1)T_{mod}]=qT_{mod}\ ,$$
$$\text{with } a+b=p\ . \quad (9)$$

The synchronization between curvature maxima and light maxima takes place in a certain rhythm of kT_{mod} and $(k-1)T_{mod}$. After q light periods, a certain pattern of curvature changes repeats itself. The number of curva-

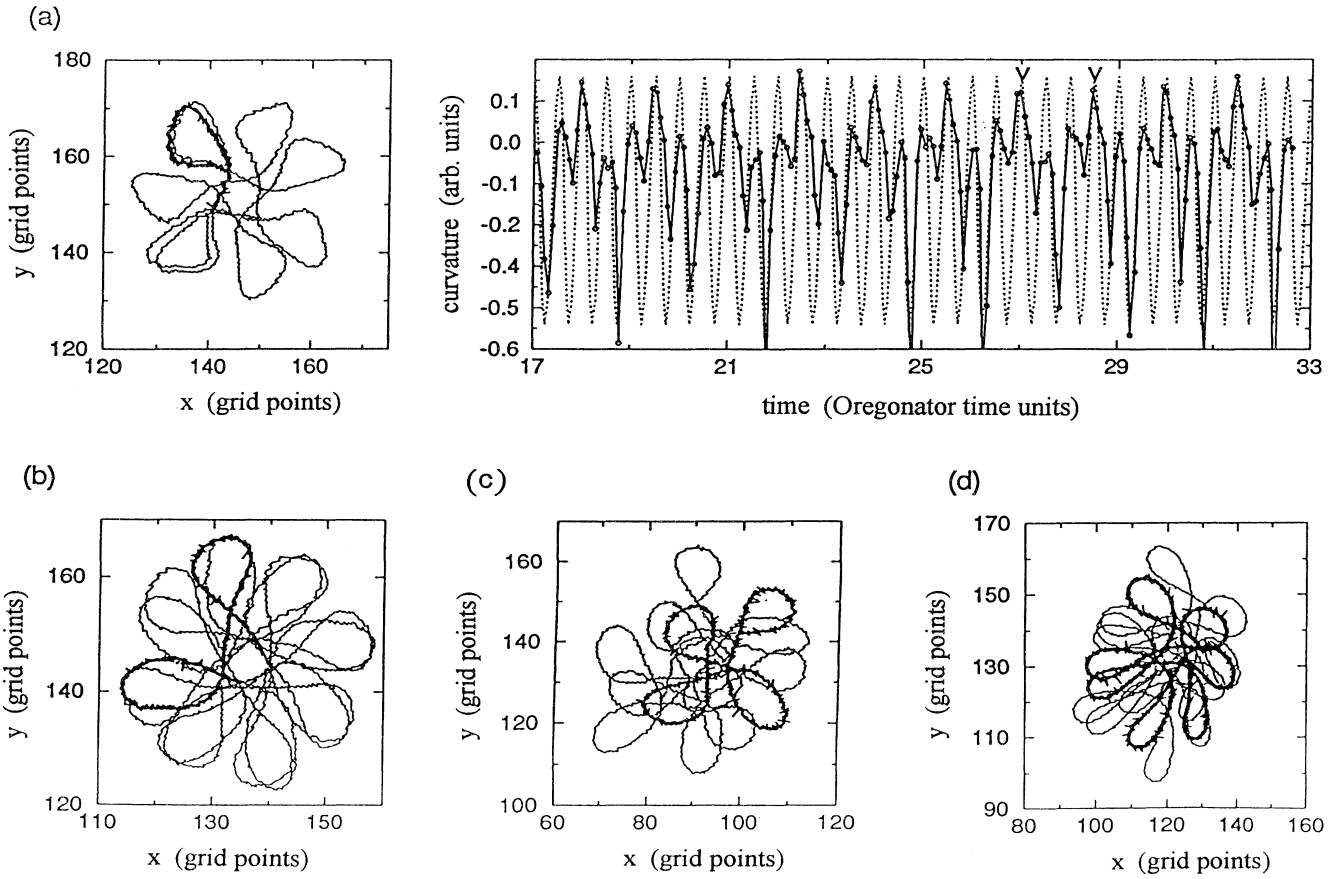

FIG. 2. Illustration of the composition of meander flowers in terms of the locking ratio $p/q=T_{mod}/T_{loop}$, as described in the text. (a) Curvature time series in comparison to the periodically changing light intensity (dashed curves with arbitrary amplitude) and patterns for $f=2.7$, $a=0.008$, $T_{mod}=0.5$, $p/q=1/3$. Tip path patterns for (b) $f=3.0$, $a=0.004$, $T_{mod}=0.6$, $p/q=2/5$, (c) $f=2.5$, $a=0.004$, $T_{mod}=0.65$, $p/q=4/9$, (d) $f=3.0$, $a=0.004$, $T_{mod}=0.9$, $p/q=7/12$. The thick lines mark the reoccurring substructure of the patterns. The corresponding part in the curvature time series is indicated by arrows.

ture peaks in this pattern p corresponds to the overall number of petals in this reoccurring substructure of the flower. The mixing components a and b determine the number of petals of similar shape and size occurring in this substructure.

Figures 2(a)–2(d) illustrate this synchronization mechanism. In Fig. 2(a) the curvature time series are shown in comparison to the external modulation. Examples taken from different computed parameter sets, i.e., different f values and forcing amplitudes, are shown with increasing complexity. The first example is obtained with large forcing amplitude $a=0.008$, where curvature changes are more pronounced. The remaining examples are calculated with $a=0.004$. The corresponding tip path patterns are shown next to the time series, and substructures are indicated by a thick line. The first example is a *simple flower* corresponding to the mode-locked state $p/q=1/3$. All petals have the same shape, and the corresponding curvature peak repeats after three modulation periods. The next flower shown consists of two petals with different shapes corresponding to $2T_{\mathrm{mod}}$ and $3T_{\mathrm{mod}}$ alternating, so that the locking ratio 2/5 is represented by $2T_{\mathrm{loop}}=1(2T_{\mathrm{mod}})+1(3T_{\mathrm{mod}})=5T_{\mathrm{mod}}$. In Fig. 2(c) the subflower has four petals, where three are equally shaped; here $4T_{\mathrm{loop}}=3(2T_{\mathrm{mod}})+1(3T_{\mathrm{mod}})=9T_{\mathrm{mod}}$. While the former examples occurred at locking ratios between 1/3 and 1/2, that is, $k=3$ as defined before, the last one is a more complex example for $k=2$. Here it is $p/q=7/12$, and the subflower is made up of seven petals. Five of them form in a period of $2T_{\mathrm{mod}}$, and the remaining two in $1T_{\mathrm{mod}}$. Therefore, we have $7T_{\mathrm{loop}}=5(2T_{\mathrm{mod}})+2(1T_{\mathrm{mod}})=12T_{\mathrm{mod}}$. In the corresponding curvature time series [not shown in Fig. 2(d)] the same curvature pattern repeats after 12 modulation periods.

In all cases the substructure reoccurring after a multiple of T_{mod} could be identified with a certain number of petals that repeat in form and shape; only their position and orientation in space differ. Thus, even very complicated-looking flowers seem to be highly ordered. Note also that the mixing components (a,b) determine the position of the rational number p/q in the Farey tree with respect to $1/k$ and $1/(k-1)$, in between which they occur. A similar ordering structure has been previously observed in a semiconductor model for self-generated current oscillations [31,32].

Mode-locked states are typically expected to be separated by quasiperiodic behavior for small forcing amplitudes. In contrast to phase locking, quasiperiodic behavior generally manifests itself in varying phase differences between the forcing period and the curvature period. We also found *irregular* patterns in which there is no observable reoccurring structure in the curvature time series that synchronizes with the external forcing after a certain number of time steps (2^{16}). However, single peaks do synchronize with the light, while the amplitude and form of the peaks changes in some irregular way.

B. Behavior on the major entrainment bands

Just before the 1/1 entrainment band, regular subflowers develop, composed of more and more petals that are shifted in space and connected by a different sized connection loop. The number of petals making up the subflower monotonically increases approaching the 1/1 band. More and more peaks in the curvature time series are totally synchronized with the forcing period, while one differently shaped peak corresponds to $2T_{\mathrm{mod}}$. Figure 3 depicts tip path patterns for two different modulation periods close to the beginning of the entrainment band.

As the beginning of the band is finally reached, the connection loop disappears. The flower no longer moves (since $f_2=f_3$), and consists of equal sized petals. The curvature variations occur absolutely synchronously with the forcing period, i.e., there is no phase difference at the very beginning of the band (see Fig. 4). Once on the band, the difference between the two remaining frequencies f_1 and f_2 and the amplitude of f_2 increase with further increase of T_{mod}, resulting in flowers with more and more petals on a larger radius. The sizes of the petals (meaning the enclosed area) stay approximately the same as those determined by T_{loop} at the beginning of the band, where the radii of f_1 and f_2 coincide. Only the distance between them changes linearly with T_{mod}, so that $T_{\mathrm{mod}}=T_{\mathrm{loop}}$ is satisfied on the whole band. Qualitatively, the same behavior was observed experimentally

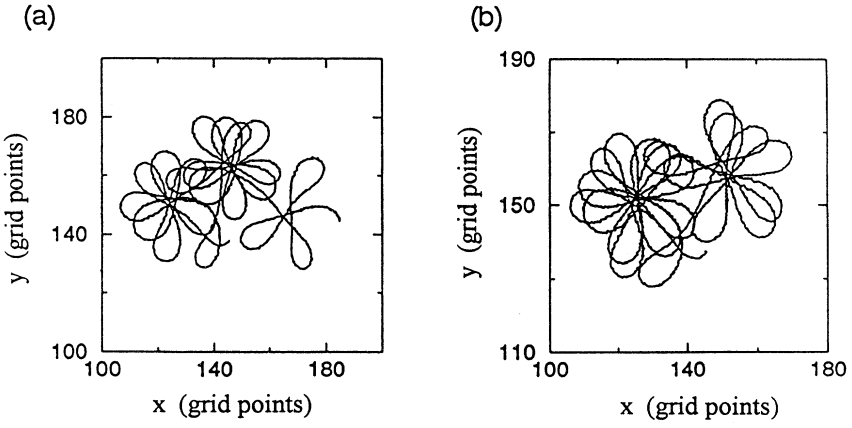

FIG. 3. Curvature time series and tip path patterns described as connected subflowers just before the beginning of the 1/1 entrainment band calculated with $f=3.0$, $a=0.004$. The modulation periods are (a) $T_{\mathrm{mod}}=1.25$ and (b) $T_{\mathrm{mod}}=1.27$ in Oregonator time units.

with the light-sensitive BZ medium [9]. The simple flowers belonging to the 1/2 and 1/1 entrainment bands have been shown in Fig. 3 of Ref. [9].

The development on the band can also be followed in the curvature time series in the following way: The curvature peaks lose their smoothness from the beginning of the band (where they might be approximated by $\sin^2$) and change their shapes, such that harmonics of T_{loop} develop that are the more pronounced the larger the forcing amplitude. In addition, the synchronization between curvature maxima and light maxima takes place with a constant phase shift, which increases with T_{mod} towards the end of the band, where it approaches π, as shown in Fig. 4.

In the case of not-too-large forcing amplitudes, the 1/1 entrainment band terminates with a period doubling. Figure 5 shows the tip path Fourier spectra at the end of the 1/1 band. Figure 5(a) corresponds to the last pattern found on the band for $f=2.5$ and $a=0.004$. The sharp, large amplitude peak corresponds to f_2. It can be clearly seen in 5(b) and 5(c) that this peak begins to split just beyond the band, causing the flower to move again and to develop a substructure.

Analogous behavior is observed at the end of the 1/2 band. While here curvature peaks corresponding to one petal appear to split such that new structures and different petal forms occur, additional peaks seem to occur at the end of the 1/1 band causing the new substructure to develop inside the large radius pattern. This can be clearly seen in Fig. 5(b). In both cases pronounced harmonics of T_{loop} develop towards the end of the band and the amplitude of the curvature peaks is modulated when the end of the band is reached.

With further increase of T_{mod} beyond the 1/1 band, the substructure is more often repeated until it dominates the whole flower. The original structure from the end of the band is still present, but now takes over the role of forming the connection loops for the more pronounced substructure. Thus, the basic components of this complex flower have changed their roles.

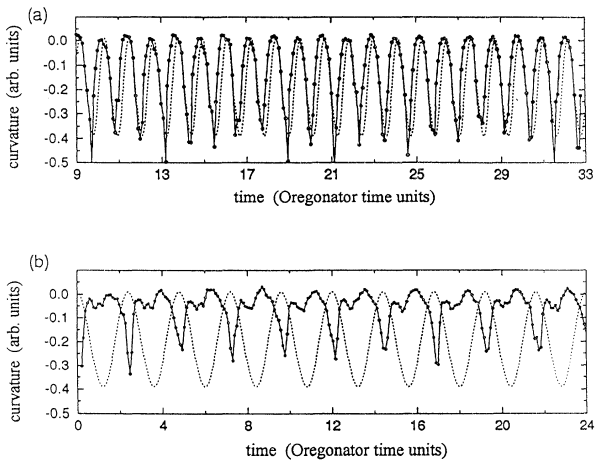

FIG. 4. Synchronization between external modulation and path curvature with negligible phase shift at the beginning of the 1/1 entrainment band (a) $T_{\text{mod}}=1.15$, which increases up to π close to the end of the band (b) $T_{\text{mod}}=2.4$ for $f=2.7$ and $a=0.008$.

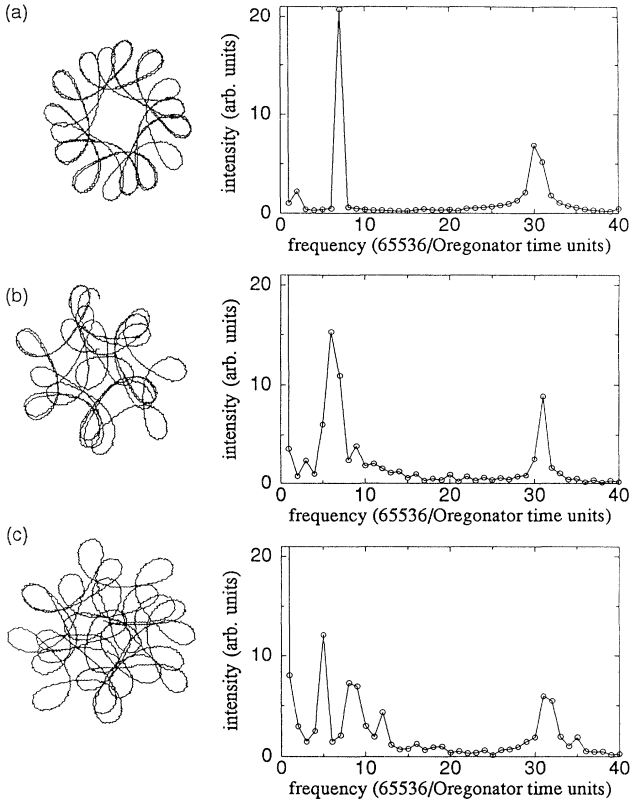

FIG. 5. Tip trajectories and corresponding Fourier spectra at the end of the 1/1 entrainment band for $f=2.5$ and $a=0.004$ (a) $T_{\text{mod}}=1.75$, (b) $T_{\text{mod}}=1.78$, (c) $T_{\text{mod}}=1.80$.

For the same small forcing amplitude, the size and number of petals of the last flower in the band depend on the choice of f. The more petals (that is, the larger the ratio T_2/T_{loop}) in the underlying unforced meander pattern, the more petals will this last flower contain. However, the width of the major entrainment bands is approximately the same in both investigated cases for $a=0.004$; the bands are simply moved on the T_{mod} axis.

For a larger forcing amplitude, the transition between the 1/2 and 1/1 bands occurs abruptly with no additional mode-locked states in between. Such a behavior has necessarily to go along with a resonance. We observe bistable behavior between the 1/2 and 1/1 bands and a termination of the bands with a resonance in T_1.

In the following we discuss the overlap region and the end of the 1/1 entrainment band in terms of the basic frequencies and compare it to resonance conditions in the unforced case. It has been previously shown that the unforced Oregonator exhibits a resonance in T_1, resulting in drifting spirals when the parameter f is varied for some fixed ϵ [14,27]. In this case the secondary frequency f_2 approaches zero with infinite amplitude, $f_2=0$ and $f_1=f_{\text{loop}}$. For smaller values of ϵ it has been found that

the epicycle frequencies approach each other with increasing values of the excitation threshold. However, a resonance between f_1 and f_2 is prevented by the onset of the so-called hypermeander [14,15], which introduces a third frequency into the system (for a more detailed discussion, see [27]). Thus $f_1=f_2$, which is equivalent to $T_1=2T_{\text{loop}}$, meaning that the tip of the spiral performs two loops during one rotation with an angle π between the petals, cannot exist in a two-frequency regime.

Under large amplitude periodic forcing we find similar conditions at the end of the major entrainment bands. On the 1/2 band $T_{\text{mod}}=1/2T_{\text{loop}}$ holds per definition. With increasing T_{mod} we find f_2 continuously decreasing with increasing amplitude. When f_2 reaches zero we have $f_{\text{loop}}=f_1=1/2f_{\text{mod}}$, thus a resonance between T_{loop} and T_1 and a 1/2 resonance between T_{mod} and T_1. But at the same time, harmonics of T_{loop} have developed. On the 1/2 band the second harmonic of T_{loop} corresponds to T_{mod} and the band terminates when the second harmonic reaches the same amplitude as that of T_{loop}. Then T_{mod} becomes T_{loop}, the period of curvature changes, and f_2 and $f_3=f_{\text{mod}}-f_1$ have changed their roles. Thus the termination of the 1/2 band can also be viewed as a resonance between $T_{\text{mod}}=T_{\text{loop}}$ and T_1, which determines the beginning of the 1/1 band. Approaching the resonance point from the opposite direction means that $f_3=f_2$ is progressively decreasing in amplitude and approaching f_1 until they coincide. Then the resonance condition reads $T_1=2T_{\text{loop}}$. As mentioned before this is an unstable condition and a "down jump" to the 1/2 band occurs while T_{mod} and T_{loop} exchange their roles.

Tip path patterns corresponding to this overlap region obtained for different initial conditions are shown in Fig. 6. Figure 7 depicts the "down jump" in terms of the x and y coordinates of the spiral's tip as a function of time. The large radius patterns close to the end of the 1/2 band

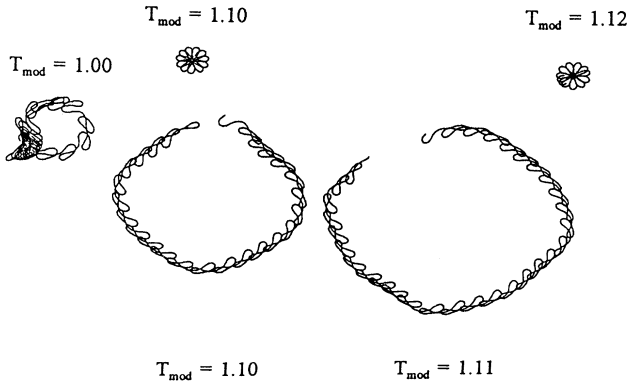

FIG. 6. Tip trajectories in the bistable region where the entrainment bands overlap, obtained for different initial conditions with $f=2.7$, $a=0.008$. Small patterns belong to the 1/1 band and large radius patterns to the 1/2 band. The very left pattern corresponds to the "down jump," where the transition from the 1/1 band to the 1/2 band occurs. The initial spiral has been calculated on the 1/1 band with slightly larger T_{mod}.

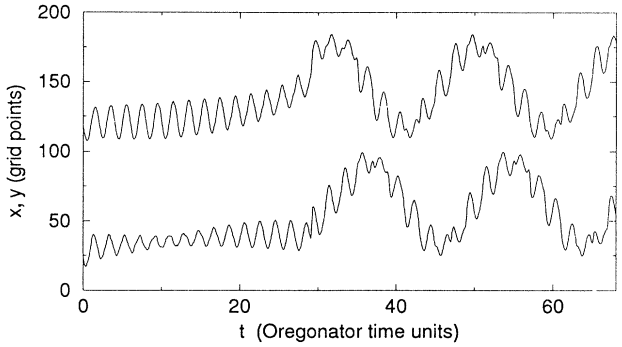

FIG. 7. The transition between the 1/1 entrainment band and the 1/2 band in the bistable region for $f=2.7$, $a=0.008$ and $T_{\text{mod}}=1.0$. x and y coordinates of the spiral's tip versus time.

suggest that the angle between the petals is indeed approaching π.

The scenario at the end of the 1/1 band seems similar. A harmonic of T_{loop} is growing again and f_2 approaches zero. However, now, we do not have a third frequency that could help change its role, since it is $f_2=f_3$ on the 1/1 band and both frequencies simultaneously approach zero.

The resonance condition reads identical to the straight looping line drift in the unperturbed case. The difference, however, is that here additional curvature changes develop such that the core of the spiral is not traveling along a straight line, but the sign of the curvature is changed in between the loops. The curvature sign changes become more pronounced while the spiral is traveling longer distances between the loops approaching the end of the band. We observe additionally that there exists a location on the spiral arm that becomes so thin that the spiral breaks up. For slightly increased T_{mod} beyond the resonance both frequencies are expected to occur with inverted sign. We could never observe a pattern corresponding to such a kind of inward meandering but instead a new instability occurs, causing the spiral to break.

Figure 8 illustrates the breaking spiral wave. The possibility of a numerical artifact has been weakened by decreasing the grid spacing down $\Delta h=0.075$ and increasing the box size to 560×560 meshes. The breakup detected in a range of T_{mod} between 2.4 and 2.85 was not influenced.

Instabilities that result in the breakup of the spiral wave have also been observed in an unperturbed system, e.g., in a model for the CO oxidation on a platin surface [37] and in electrophysiological models [38]. We find a breakup of spiral waves for the first time in a system with S-shaped, i.e., smooth nullclines.

Usually the breakup is associated with the condition that the spiral's rotation period falls below a certain T_{min} where pulse propagation becomes unstable. The unforced Oregonator model does not support this condition. However, note that under periodic perturbation the rotation period T_1 experiences a major change at the end of the 1/1 entrainment band.

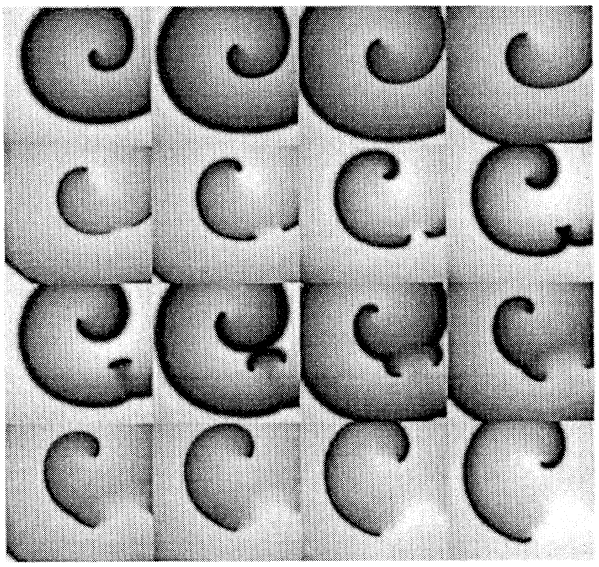

FIG. 8. Consecutive images of the inhibitor concentration at the spiral breakup separated by 0.3 Oregonator time units. The end of the 1/1 entrainment band is approached with decreasing T_{mod} for $f=2.7$, $a=0.008$ and $T_{\mathrm{mod}}=2.85$.

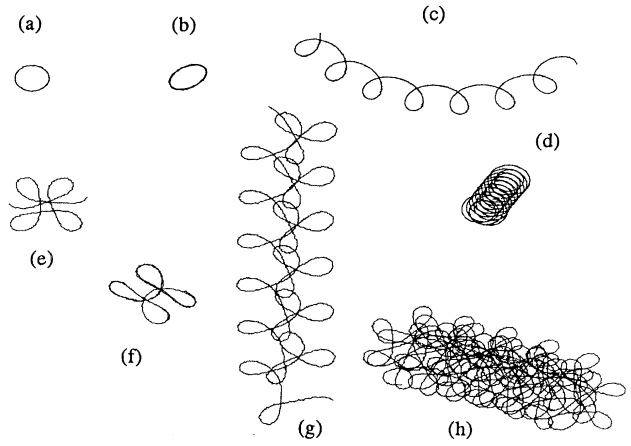

FIG. 9. Resonance response of the rotation period T_1 under periodic perturbation of rigidly rotating spirals (b)–(d) and meandering spirals (f)–(h). The unperturbed patterns are depicts in (a) $f=1.5$ and (e) $f=2.5$. The forcing amplitude is $a=0.004$ in (b),(c),(f),(g) and $a=0.008$ in (d) and (h). Closed tip path patterns are obtained in the case $T_{\mathrm{mod}}/T_1=1/2$ (b) and (f). Resonance drift of the spiral wave occurs, if $T_{\mathrm{mod}}/T1=1/1$ (c),(g) or $T_{\mathrm{mod}}/T_1=2/1$ (d),(h). The modulation periods are (b) $T_{\mathrm{mod}}=0.83$, (c) $T_{\mathrm{mod}}=1.70$, (d) $T_{\mathrm{mod}}=3.33$, (f) $T_{\mathrm{mod}}=1.00$, (g) $T_{\mathrm{mod}}=2.075$, and (h) $T_{\mathrm{mod}}=4.24$.

C. Resonances and drifting spirals

Resonances between T_{mod} and T_1 bring some additional structures into this three-frequency system. Complex meander patterns can be classified as those before and after a certain resonance, in addition to the ordering of the mode-locked states. The particular behavior, found for large forcing amplitudes, has been discussed in the preceding section. Here we draw attention to the more general cases, where the resonances lie outside the major entrainment bands.

Resonances that result in drifting spirals have been observed for the first time experimentally by Agladze, Davydov, and Mikhailov [33]. As already mentioned, they have also been found in the meander regime of unforced spirals by varying the excitability parameters [14]. Higher order resonances have been predicted [21] but not yet observed in a system of partial differential equations.

The kinematical theory developed by Mikhailov *et al.* [34,35] predicts resonances under periodic modulation of the critical curvature $K_{\mathrm{cr}}(t)=K_{\mathrm{cr}}+K_1\cos(\omega_1 t+\phi)$. Spirals drifting along a straight line were found in the cases $\omega_1/\omega_0=1/1$ and $\omega_1/\omega_0=1/2$, where ω_0 is the rotation frequency of the rigidly rotating spiral and ω_1 is the forcing frequency. In the cases $\omega_1/\omega_0=n/1$, closed n-times deformed trajectories, in particular, a closed ellipse for the forcing frequency twice that of the eigenfrequency, were found [36].

Very similar tip trajectories are found by perturbing rigidly rotating spirals in the Oregonator model. Figure 9 depicts the resonances $T_{\mathrm{mod}}/T_1=1/2$, 1/1, and 2/1, in comparison of perturbed rigidly rotating spirals to the cases found under periodic modulation of meandering spirals.

Figure 9(g) corresponds to the 1/1 resonance and illustrates that the spiral is drifting exactly along a straight line with constant velocity, while the tip is still meandering. This resonance goes along with a generalized outward-inward meandering transition, similar to the one found in the unperturbed case [14,27]. Figure 10 shows this transition with increasing T_{mod}. Here, it is not a single petal that turns its point of maximum curvature inside the larger circle, but a whole *subflower* that turns around in the following way: As described above, tip trajectories belonging to some mode-locked state are composed of petals with two different shapes and sizes (corresponding to the harmonics of T_{mod}). If there is just one petal of a certain size in the subflower among many others of the other size, we call the one *connection loop.*

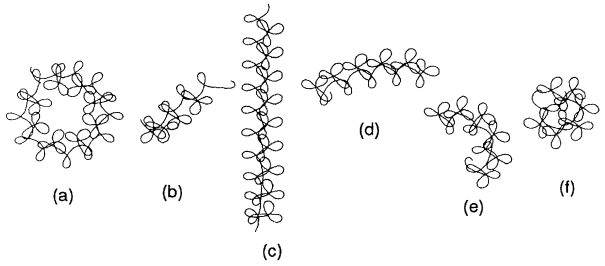

FIG. 10. Illustration of the generalized outward-inward meandering transition for $f=2.5$ and $a=0.004$ with increasing modulation period from left to right. (a) $T_{\mathrm{mod}}=2.0$, (b) $T_{\mathrm{mod}}=2.05$, (c) $T_{\mathrm{mod}}=2.075$, (d) $T_{\mathrm{mod}}=2.1$, (e) $T_{\mathrm{mod}}=2.15$, and (f) $T_{\mathrm{mod}}=2.2$.

Very similar pictures have been obtained experimentally [8,9]. This 1/1 resonance drift has also been found numerically by Zykov, Steinbock, and Müller [28], using the same model in a different parameter regime. However, note that the forcing amplitudes we allied are still large compared to the one chosen in [28]. That is why resonance drift and mode locking do not exclude each other in our observations.

The 2/1 resonance [Fig. 9(h)] is structurally equivalent to the 1/1 one just described. However, the drifting patterns are of a greater order of complexity. What we named subflower before is now the original whole flower that is drifting. The drift velocity is comparably smaller.

A qualitatively different case presents itself in that of the 1/2 resonance, which corresponds to the $\omega_1/\omega_0=n/1$ situation in the kinematical equations, where no drifting patterns were found [36]. For $f=2.5$ the 1/2 resonance [Fig. 9(f)] happens to coincide exactly with a locked state $T_{\text{mod}}/T_{\text{loop}}=2/3$. All three frequencies form integer ratios to each other, $T_{\text{loop}}/T_1=3/4$ and $T_2/T_{\text{loop}}=4$. The resulting pattern consists of four petals and remains exactly closed during 2^{17} time steps. It resembles two halves of an ellipse intersecting each other, connected by almost straight lines, such that the angle between two of the petals is close to π. It could be compared to the twice deformed circle; that is, the ellipse shown in Fig. 9(b); here a four-petaled meander flower, might be deformed twice.

V. SUMMARY

Periodic forcing has been applied in the meander regime of compound rotation. The dependence of the response of the system on a modulation period has been investigated for different forcing amplitudes and three different values of the parameter determining the excitation threshold. Mode locking of the tip path curvature period into rational multiples of the forcing period and resonance response of the rotation period have been found in qualitative agreement with experimental observations. In addition, a general scenario of the response to an increasing modulation period has been developed, which allows characterization of the observed meander pattern. The structure of complex patterns outside the major entrainment bands was found to obey the hierarchic ordering of the Farey tree. Curvature changes, and therefore the petal structure, could be expressed in terms of linear combinations of the modulation period. This structure also provides insights for the termination of the dominant entrainment bands for small forcing amplitudes, which were found to go along with a period doubling. A generalized transition from outward to inward meandering patterns accompanied by a resonance in the rotation period have been found and could be interpreted in terms of the characteristic frequencies. The resonance behavior resulting in drifting spirals and deformed closed patterns was partly found to be direct generalizations of the behavior of rigidly rotating spirals subjected to periodic forcing as predicted by the kinematical theory. For large forcing amplitude, new phenomena have been discovered. These are a bistable region caused by the overlap of entrainment bands and a new instability resulting in the breakup of the spiral. In general, the termination of the major entrainment bands was found to coincide with resonances in the rotation period, which appears to be the origin of these phenomena.

Many open questions still remain. For example, the exact mechanism causing the spiral breakup is unexplained. Furthermore, interesting irregular behavior still influenced by the forcing has been observed, such as the switching between different locked modes, which may be worth further investigation. The question of whether chaos occurs in some cases or not could also not be clarified within the scope of this work.

We stress that phenomena, such as entrainment, resonance, spiral breakup, etc., are generic features and should be observable in excitable media of quite a different nature when a periodic external forcing is applied. On the other hand, the Fitz–Hugh-Nagumo or the Barkley model certainly exhibit the same behavior as the Oregonator equations. Simulations based on this models would lead to qualitatively similar results. Our choice of the two-variable Oregonator model is motivated by several advantages that BZ systems offer for our experimental work, especially when the light-sensitive catalyst rutheniumbipyridyl is immobilized in a gel matrix. In recent years we have developed a technique to control wave propagation in this system by optical manipulation [39,8]. Although pronounced entrainment bands, resonance, and spiral breakup could be unambiguously identified experimentally with the light-sensitive medium, currently open questions remain concerning the experimental verification of all predictions obtained from the simulations. To proceed in this direction, an open reactor will be used. For the BZ system the Oregonator model is still considered as a suitable starting point to describe wave dynamics, despite the fact that the model fails to explain several experimental observations and represents great simplification compared to the complicated chemical mechanism involving a great number of kinetic steps. This is also true concerning the additional bromide flow produced photochemically to account for the photosensitivity of the system in a simplifying manner. However, we emphasize again that the main results we are reporting in this paper should be robust against the choice of a particular excitable medium or model.

In general, the behavior of meandering spirals under periodic forcing exhibits many features unseen in unperturbed systems. However, some of these patterns could be explained as generalizations of behavior known from the bifurcation structure of the unperturbed system or perturbed rigidly rotating spirals.

ACKNOWLEDGMENTS

This work was partially supported by a grant from the Deutsche Forschungsgemeinschaft and the Fonds der Chemischen Industrie.

[1] A. T. Winfree, *When Time Breaks Down* (Princeton University Press, Princeton, 1987).
[2] G. Gerisch, Naturwissenschaften **58**, 430 (1971).
[3] J. D. Lechleiter and D. E. Clapham, Science **252**, 123 (1991).
[4] S. Jakubith, H. H. Rotermund, W. Engel, A. von Oertzen, and G. Ertl, Phys. Rev. Lett. **65**, 3013 (1990).
[5] A. N. Zaiikin and A. M. Zhabotinsky, Nature **225**, 535 (1970).
[6] A. T. Winfree, Science **175**, 634 (1972).
[7] M. Braune and H. Engel, in *Selforganization and Life (ECAL'93),* edited by J. L. Denenbourg, S. Goss, G. Nicolis, H. Bersini, and R. Dagonnier (Université Libre de Bruxelles, Brussels, 1993).
[8] M. Braune and H. Engel, Chem. Phys. Lett. **211**, 534 (1993).
[9] M. Braune, A. Schrader, and H. Engel, Chem. Phys. Lett. **222**, 358 (1994).
[10] O. Steinbock, V. Zykov, and S. C. Müller, Nature **366**, 322 (1993).
[11] H.-J. Krug, L. Pohlmann, and L. Kuhnert, J. Phys. Chem. **94**, 4862 (1990).
[12] S. Skinner and H. L. Swinney, Phys. D **48**, 1 (1991).
[13] D. Barkley, M. Kness, and L. S. Tuckerman, Phys. Rev. A **42**, 2489 (1990); D. Barkley, Phys. Rev. Lett. **68**, 2090 (1992).
[14] W. Jahnke and A. T. Winfree, Int. J. Bifurc. Chaos **1**, 455 (1991).
[15] A. T. Winfree, Chaos **1**, 303 (1991).
[16] W. Jahnke, W. E. Skaggs, and A. T. Winfree, J. Phys. Chem. **93**, 740 (1989).
[17] M. Braune and H. Engel, Chem. Phys. Lett. **204**, 257 (1993).
[18] S. C. Mueller, T. Plesser, and B. Hess, Science **230**, 661 (1985).
[19] T. Plesser, S. C. Mueller, and B. Hess, J. Phys. Chem. **94**, 7501 (1990).
[20] S. C. Mueller and T. Plesser, in *Chemical Waves and Patterns,* edited by R. Kapral and K. Showalter (Kluwer Academic, Dordrecht, 1995).
[21] D. Barkley, Phys. Rev. Lett. **72**, 164 (1994).
[22] E. Lugosi, Phys. D **40**, 331 (1989).
[23] E. Meron, Phys. D **49**, 98 (1991).
[24] A. Karma, Phys. Rev. Lett. **65**, 2824 (1991).
[25] J. J. Tyson, in *Oscillations and Traveling Waves in Chemical Systems,* edited by R. J. Field and M. Burger (Wiley, New York, 1985), pp. 93–144.
[26] L. Kuhnert, Naturwissenschaften **73**, 96 (1983).
[27] A. Schrader, diploma thesis, Technische Universität Berlin, 1994.
[28] V. Zykov, O. Steinbock, and S. C. Müller, Chaos **4**, 509 (1994).
[29] H. G. Schuster, *Deterministic Chaos* (VHC, Weinheim, 1988).
[30] M. H. Jensen, P. Bak, and T. Bohr, Phys. Rev. A **30**, 1960 (1984).
[31] U. Rau, J. Peinke, J. Parisi, R. P. Huebner, and E. Schöll, Phys. Lett. A **124**, 335 (1987).
[32] H. Naber and E. Schöll, Z. Phys. B **78**, 305 (1990).
[33] K. I. Agladze, V. A. Davydov, and A. S. Mikhailov, Pis'ma Zh. Eksp. Teor. Fiz. **45**, 601 (1987) [JETP Lett. **45**, 767 (1987)].
[34] A. S. Mikhailov, in *Foundation of Synergetics I* (Springer-Verlag, Berlin, 1990).
[35] A. S. Mikhailov, V. S. Zykov, and V. A. Davydov, Physica D **70**, 1 (1994).
[36] N. Gottschalk, Studienarbeit, Technische Universität Berlin, 1993.
[37] M. Bär and M. Eiswirth, Phys. Rev. E **48**, R1635 (1994).
[38] A. Karma, Phys. Rev. Lett. **71**, 1103 (1993).
[39] H. Engel and M. Braune, Phys. Scr. **49**, 685 (1993).

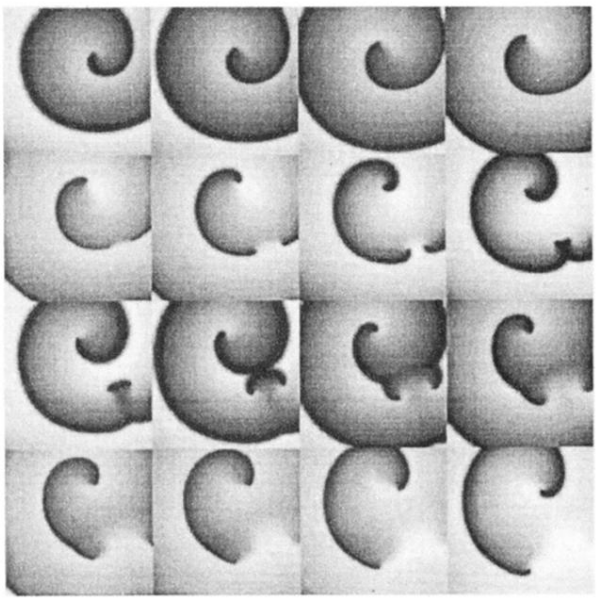

FIG. 8. Consecutive images of the inhibitor concentration at the spiral breakup separated by 0.3 Oregonator time units. The end of the 1/1 entrainment band is approached with decreasing T_{mod} for $f=2.7$, $a=0.008$ and $T_{\mathrm{mod}}=2.85$.